Supplementary Information

Different Phosphorylation and Farnesylation Patterns Tune Rnd3-14-3-3 Interaction in Distinct Mechanisms

Jun Hu, Xue-Meng Sun, Jing-Yun Su, Yu-Fen Zhao, Yong-Xiang Chen*

Key Laboratory of Bioorganic Phosphorus Chemistry and Chemical Biology (Ministry of Education),

Department of Chemistry, Tsinghua University, Beijing 100084, China

*Corresponding Author: Assoc. Prof. Dr. Yong-Xiang Chen, E-Mail: chen-yx@mail.tsinghua.edu.cn

Contents

1. Materials and Methods

Reagents

Amino acids, coupling reagents, solvent and other reagents for peptide synthesis were purchased from Gil Biochemical (Shanghai) Co., LTD, Beijing Enokai Technology Co., LTD, J&K Scientific and Acros Organics.

Peptide Synthesis

All the peptides were obtained through Fmoc solid-phase peptide synthesis (SPPS) on the basis of strategy we developed previously[1]. In order to generate C-terminal methyl esters, we synthesized Fmoc-Cys-OMe through a two-step reaction, which was coupled to the 2-chlorotrityl chloride resin via the thiol group at the side chain. The resultant loading was around 0.2 mmol/g. The peptides were then synthesized following the general Fmoc-SPPS strategy, and released by adding the cleavage reagents (TFA / phenol / H_2O / thioanisole / EDT / Me_2S / NH_4I = 81: 3: 5: 5: 2.5: 2: 1.5). As for fluorophore-labeled peptides, a short polyethylene glycol linker was attached to the N-terminal amino acid of peptides and 5(6)-carboxyfluorescein (FAM) was then attached to the linker. All the released peptides were purified by Shimadzu semi-preparative HPLC with LC-20A as solvent pumps. The column type is YMC-Pack ODS-A (250 x 20 mm, YMC Co., Ltd, Japan) and the flow rate we used was 10 mL/min. The purity and accuracy were measured by analytic HPLC (YMC-Pack ODS-A column (150 x 4.6 mm, YMC Co., Ltd, Japan) at flow rate of 0.8 mL/min) and ESI-MS (SYNAPT G2-Si HDMS system (Waters Corporation) or Esquire-LC ion trap mass spectrometer system (Bruker Corporation)) (Fig. S1-S6). The farnesylated or geranylgeranylated peptides were produced via one-step reaction by treating the released peptides with *trans, trans*-farnesyl bromide or geranylgeranyl bromide (synthesized as previous article[2]) and $Zn(OH)_2$, and then purified by preparative HPLC.

14-3-3ζ Expression

In order to generate 14-3-3ζ without additional tag, the 14-3-3ζ gene was cloned into the pTWIN1 Vector (New England Biolabs Inc.) before the gene of intein-CBD. For higher cutting efficiency, we inserted glycine at the end of 14-3-3ζ (The last amino acid on 14-3-3ζ is asparagine, which is hardly cleaved when it is adjacent to the intein[3]).The designed primers are showed in table 2,The constructed plasmid was transformed into BL21 (DE3) competent *E. coli* (New England Biolabs Inc.) and expressed. The 14-3-3ζ-intein-CBD fusion protein was purified using chitin beads (New England Biolabs Inc.). After the beads were treated by 200 mM β-mercaptoethanol (βME) overnight[3], 14-3-3ζ without tag was released. Its purity and integrity were verified by SDS-PAGE and mass spectrum (Fig. S7).

Photo-Induced Cross-Linking of 14-3-3ζ

In this experiment[4], we prepared solution A: ammonium persulfate (20 mM in water), solution B: tris (2, 2'-bipyridyl) dichlororuthenium(II) hexahydrate (1 mM in water) and solution C: dithiothreitol (1 M in water). In order to trigger the cross-linking, we mixed 10 μL 20 μM protein, 2 μL solution A and 2 μL solution B by vortex, and centrifuge the mixture for 5 seconds, then exposed the mixture incandescent lamp (220V, 40W) in very close distance for different illumination time (3 s, 6 s, 9 s, 15 s, 30 s). 2 μL solution C was added to the mixture to stop the reaction. The final solutions were applied for the SDS-PAGE immediately (Fig.S8).

SDS-PAGE and Native-PAGE

Sodium dodecyl sulfate polyacrylamide gel electrophoresis (SDS-PAGE) was used for the identification of protein purity and molecular weight.In the electrophoresis system, sodium dodecyl sulfate (SDS) and the strong reductant (such as mercaptoethanol, dithiothreitol, etc) were added. These reagents lead protein conformation changes and break it down into subunits. A variety of ingredients used in a gel : 0.5 M Tris-HCl (pH 6.8), 1.5 M Tris(pH = 8.8), 10% (w/v) SDS, Acrylamide/Bis-acrylamide (30%/0.8% w/v), 10% (w/v) ammonium persulfate (AP), tetramethylethylenediamine (TEMED).

Native PAGE was used for the detection of 14-3-3ζ dimer. 14-3-3ζ were prepared in a non-reducing non-denaturing sample buffer and gel was prepared with 0.375 M Tris-HCl (pH = 8.8), Acrylamide/Bis-acrylamide (30%/0.8% w/v), 62.5 mM Tris-HCl (pH 6.8), 10% (w/v) ammonium persulfate (AP), TEMED. Denaturants are not used in Native-PAGE, so the subunit interactions within multi-subunit proteins are retained. Because pI (isoelectric point) of 14-3-3ζ is 4.73, electrophoresis experiments were carried out as usual and it's no need to reverse the anode.

Isothermal Titration Calorimetry (ITC)

The ITC measurements were performed on a MicroCal iTC200 (General Electric Company). 14-3-3ζ and Rnd3 peptides without fluorophore were dissolved in buffer (20 mM Tris-(2-carboxyethyl)-phosphin, 150 mM NaCl, 1 mM TCEP and pH 7.5). 40 µM 14-3-3ζ was added to the ITC cell and 200~400 µM Rnd3 peptides were sucked from tubes to the syringe. All the experiments were performed at 25 °C (Total injected volume, 40 µL; reference power, 5 µCal/s; initial delay, 60 s; spacing, 150 s, stirring speed, 750 rpm). Data were analyzed using the program Origin (MicroCal).

Fluoresence Polarization (FP) Assay

The Rnd3 peptides labeled with FAM were dissolved respectively in buffer (20 mM Tris-(2-carboxyethyl)-phosphin, 150 mM NaCl, 1 mM TCEP and pH 7.5) at a concentration of 250 nM. 14-3-3ζ were added to reach different concentrations of 0, 0.1, 0.2, 0.5, 1, 2, 3, 5, 10 µM. The experiments were carried with on 96-well plates at 25 °C. The fluorescence polarization values were measured on a Synergy 4 Multi Detection Microplate Reader (BioTek Instruments, Inc.), with excitation at 444 nm and emission at 480 nm. The data were fitted using equation S1, obtaining the dissociation constant K_D.

$$y = F_{min} + \left(K_D + C + x - \sqrt{(K_D + C + x)^2 - x} \right) * 2 * (F_{max} - F_{min}) \quad \text{(Equation S1)}$$

Where y, the polarization value; x, the final concentration of 14-3-3ζ. F_{max}, maximal fluorescence polarization; F_{min}, minimal fluorescence polarization. C, the concentration of fluorescent labeled peptides.

Stopped-Flow Experiments

The binding kinetics were measured by stopped-flow apparatus coupled with fluorescence polarization detector (Hi-Tech Scientific SF-61SX2/DX2 Stopped-Flow system, TgK Scientific). 1 µM FAM-labeled peptides and different concentration of 14-3-3ζ (10, 12.5, 15, 17.5, 20 µM) were mixed, and the change of FP value with time was monitored with excitation at 497 nm and emission wavelength greater than 500 nm. 1 µM FAM-labeled peptides and 10 µM 14-3-3ζ were mixed for 3 minutes, followed by the addition of 50 µM corresponding unlabeled peptide to release the FAM-labeled one. The change of FP value with time in the dissociation process was monitored. The data of the dissociation process were fitted using equation S2 to give the dissociation rate constant k_{off}. The data of monophosphorylated peptide association process were fitted using equation S3 under pseudo first-order conditions([protein]<< [ligand]) to give the association rate constant k_{on} and k_{off}.

$k_{obs} = - A * \exp(-k_{off,ov} * x + C)$ (Equation S2)

$k_{obs} = k_{on} [\text{protein}] + k_{off})$ (Equation S3)

For peptides bearing two remote phosphates epitopes or adjacent phosphate and lipid epitopes, we assumed that the binding process was a two-step reversible interaction. The group of association curves with different concentrations of 14-3-3ζ were fitting using global fit in MATLAB software. The kinetic parameters were obtained by a numerical integration of a set of differential equations describing a two-step binding mechanism (equations S4-8). For peptide 218_240pi, we first assumed pS218 initiated the binding and take k_{off} of 240pi as the $k_{d,1}$: 44.25 - 17.81< $k_{d,1}$ < 44.25 + 17.81 (This is used as a range limit to $k_{d,1}$). The rest parameters were determined by global fit and protein concentration is defined as the concentration of 14-3-3ζ dimer ([14-3-3ζ]/2). Then we assumed pS218 initiated the binding and take $2k_{on}$ of 240pi as the $k_{a,1}$: 2*(29.63 - 2.31) < $k_{a,1}$ < 2*(29.63 + 2.31) (This is used as a range limit to $k_{a,1}$). The rest parameters were determined by global fit.

For peptides 240piFar and PDE6C_pi_GG, we first assumed pS240 or PDE6C_pi initiated the binding and take k_{on} of 240pi or PDE6C_pi as the $k_{a,1}$: 29.63 - 2.31 < $k_{a,1}$ < 29.63 + 2.31 or 4.06 - 0.22 < $k_{a,1}$ < 4.06 + 0.22 (This is used as a range limit to $k_{a,1}$). The rest parameters were determined by global fit and protein concentration is defined as the concentration of 14-3-3ζ monomer. In another case, we assumed fC241 or PDE6C_GG initiated the binding and set $k_{a,1}$, $k_{d,1}$, $k_{a,2}$, and $k_{d,2}$ as unknown constants, which were determined by global fit. Finally, we analyzed the rationality of the parameters and inferred the appropriate combination model. We calculated the overall K_D and k_{off} using equations S9-10.

For multi-modified peptides, the binding is a two-step process, the derivation of the equations are as follows:

$$H \ + \ G \underset{k_{d,1}}{\overset{k_{a,1}}{\rightleftharpoons}} H\text{-}G_* \underset{k_{d,2}}{\overset{k_{a,2}}{\rightleftharpoons}} H\text{-}G$$
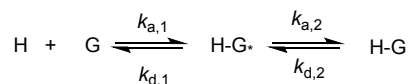
d[H] / dt = $k_{d,1}$ * [H-G*] - $k_{a,1}$ * [H] * [G]	(Equation S4)
d[G] / dt = $k_{d,1}$ * [H-G*] - $k_{a,1}$ * [H] * [G]	(Equation S5)
d[H-G*] / dt = $k_{a,1}$ * [H]*[G] + $k_{d,2}$ * [H-G] - $k_{d,1}$ * [H-G*] - $k_{a,2}$ * [H-G*]	(Equation S6)
d[H-G] / dt = $k_{a,2}$ * [H-G*] - $k_{d,2}$ * [H-G]	(Equation S7)
y = r0 * [G] + r1 * [H-G*] + r2 * [H-G] + C	(Equation S8)
$K_D = k_{d,1}*k_{d,2} / (k_{a,1} *(k_{a,2} + k_{d,2}))$	(Equation S9)
$k_{off} = k_{d,1}*k_{d,2} / (k_{d,1} + k_{a,2} + k_{d,2})$	(Equation S10)

y represents the signal we measured, the fluorescence polarization; r0 is the coefficient of fluorescence polarization value of G (fluoresce labeled peptides), r1 is the coefficient of fluorescence polarization value of H-G*, r2 is the coefficient of fluorescence polarization value of H-G, $k_{a,1}$, $k_{d,1}$, $k_{a,2}$, $k_{d,2}$, are the rate constant of the two-step binding process. For the initial fit, we set restrictions as follows: $k_{a,1}$ >0, $k_{d,1}$ >0, $k_{a,2}$ >0, $k_{d,2}$ >0, 0 < r0 <1, 0 < r1 <1, 0 < r2 <1.

Molecular Dynamics Simulation

Molecular dynamics (MD) simulation was performed by using GROMACS software. The structure of 14-3-3ζ came from its crystallographic structure in the complex with a 7-mer Rnd3 peptide (PDB code: 4bg6). The peptides structures were constructed based on the peptide structure in crystal. The coordinates of atoms is the same as the atoms in crystal, and optimize the structure of the redundant atoms on the basis of controling the main chain structure. Ambertool18 package was used to generate the force field of peptides, and the structures of three peptides were obtained. The process can now be reformulated with more detail as follows: remove unnecessary information and retain peptides residues and crystal water. At this point, the PDB structure file has only these two parts of the heavy atoms. For the late running dynamics, the work needed to be done is: hydrogenation, adding solvent (counterbalance ion and water), to produce the PRMTOP, INPCRD files needed for running dynamics. Then using acpype.py script to convert PRMTOP, INPCRD file to top, gro file which can be recognized by gromacs package. The optimal protein-peptide complex conformations were obtained by docking. Active space parameters:box center for 240pi peptide (-20.005, 7.664, 6.179), for no_piFar (-18.01, 7.395, 7.949), for 240piFar (-18.01, 7.395, 7.949); all three systems have the same box size (15, 15, 28.5). Autodock Vina software is used for flexible docking and all the three ligands set the main chain to be rigid and the side chain to be flexible. The results with the highest docking affinity were used as the initial structure of the subsequent MD simulations.The explicit solvent TIP3P model was adopted for the MD simulation. The size of the simulated box was determined according to the size of protein (the three edges of the cuboid box were all 1 nm away from the protein). Periodic boundary conditions were adopted during the simulation. The NPT (cnstant temperature, constant pressure) ensemble was used: temperature is set at 300 K, pressure at 1 atm. Temperature control algorithm is Velocity rescale, temperature coupling constant is set at 0.1 ps, z-direction, XY plane is controlled at 1 atmosphere by Berendsen Borostat algorithm, and pressure coupling constant is set at 0.1 ps. The long-range electrostatic interaction was calculated by particle mesh Ewald (PME). The cut-off radius of VDW was set as 1.2 nm. The LINCS algorithm was used to limit the bond length of water molecules. The whole system

4

started with energy minimization. Then limit the protein and ligand position to prebalance 10 ns. The final structure outputs came from 100 ns simulation without position restrictions.

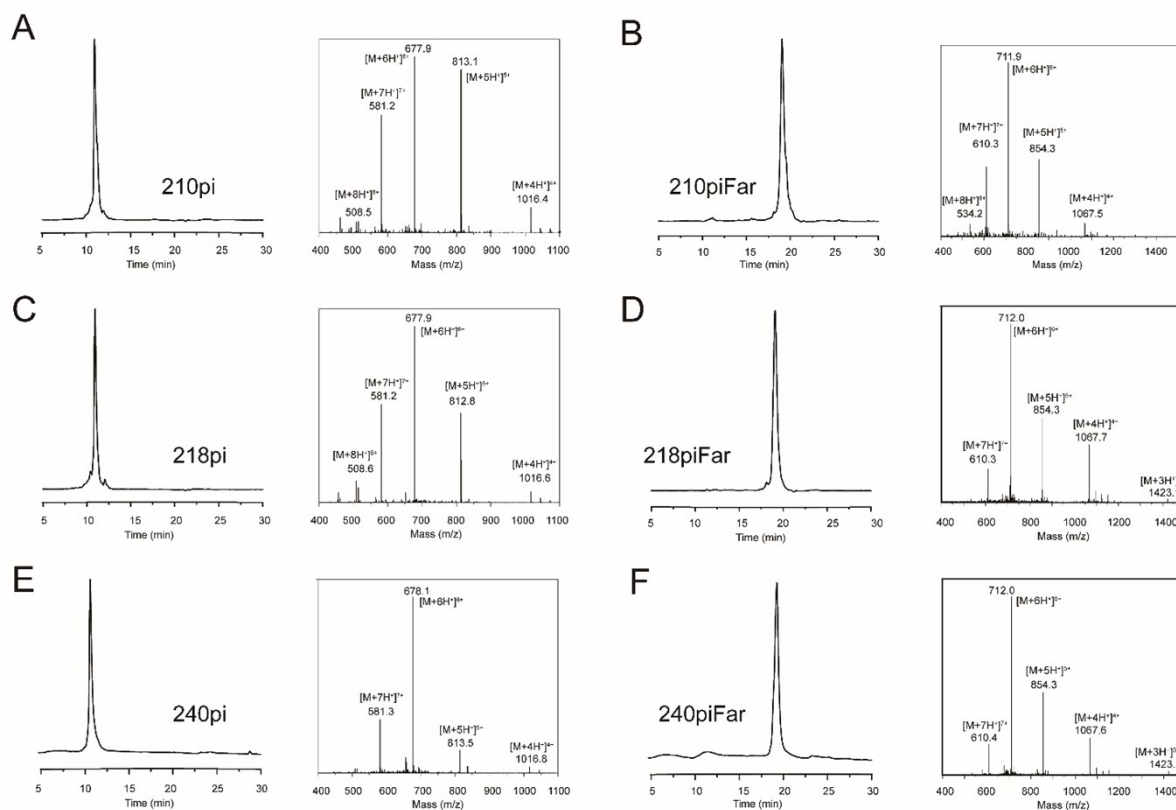## 2. Supplementary Figures and Tables

Figure S1. The analytical HPLC and ESI-MS analysis of synthesized single-phosphorylated Rnd3 peptides. All the peptides were analyzed by C18 analytical column, a gradient of 20-80% B (phase A solvent is distilled water with 0.6‰ TFA, phase B solvent is 80% acetonitrile in water with 0.6‰ TFA) for 30 min. A) 210pi. The calculated molecular mass is 4059.11 and 508.4 for $[M+8H]^{8+}$, 580.9 for $[M+7H]^{7+}$, 677.5 for $[M+6H]^{6+}$, 812.8 for $[M+5H]^{5+}$, 1015.8 for $[M+4H]^{4+}$. B) 210piFar. The calculated molecular mass is 4263.30 and 533.9 for $[M+8H]^{8+}$, 610.0 for $[M+7H]^{7+}$, 711.6 for $[M+6H]^{6+}$, 853.7 for $[M+5H]^{5+}$, 1066.8 for $[M+4H]^{4+}$. C) 218pi. The calculated molecular mass is 4059.11 and 508.4 for $[M+8H]^{8+}$, 580.9 for $[M+7H]^{7+}$, 677.5 for $[M+6H]^{6+}$, 812.8 for $[M+5H]^{5+}$, 1015.8 for $[M+4H]^{4+}$. D) 218piFar. The calculated molecular mass is 4263.30 and 610.0 for $[M+7H]^{7+}$, 711.6 for $[M+6H]^{6+}$, 853.7 for $[M+5H]^{5+}$, 1066.8 for $[M+4H]^{4+}$, 1422.1 for $[M+3H]^{3+}$. E) 240pi. The calculated molecular mass is 4059.11 and 508.4 for $[M+8H]^{8+}$, 580.9 for $[M+7H]^{7+}$, 677.5 for $[M+6H]^{6+}$, 812.8 for $[M+5H]^{5+}$, 1015.8 for $[M+4H]^{4+}$. F) 240piFar. The calculated molecular mass is 4263.30 and 610.0 for $[M+7H]^{7+}$, 711.6 for $[M+6H]^{6+}$, 853.7 for $[M+5H]^{5+}$, 1066.8 for $[M+4H]^{4+}$, 1422.1 for $[M+3H]^{3+}$.
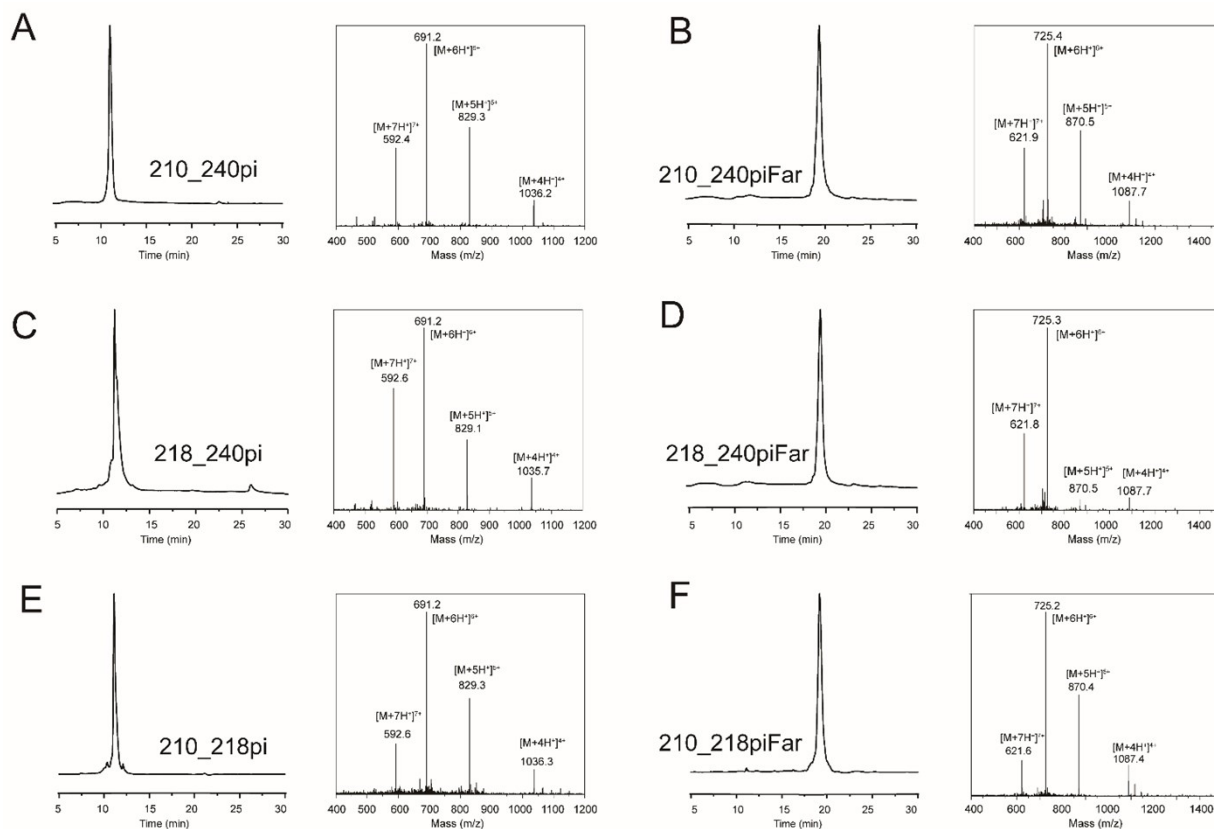
Figure S2. The analytical HPLC and ESI-MS analysis of synthesized dual-phosphorylated Rnd3 peptides. All the peptides were analyzed by YMC-Pack ODS-A column at flow rate of 0.8 mL/min) C18 analytical column, a gradient of 20-80% B (phase A solvent is distilled water with 0.6‰ TFA, phase B solvent is 80% acetonitrile in water with 0.6‰ TFA) for 30 min. A) 210_240pi. The calculated molecular mass is 4139.08 and 592.3 for $[M+7H]^{7+}$, 690.8 for $[M+6H]^{6+}$, 828.8 for $[M+5H]^{5+}$, 1035.8 for $[M+4H]^{4+}$. B) 210_240piFar. The calculated molecular mass is 4343.26 and 621.5 for $[M+7H]^{7+}$, 724.9 for $[M+6H]^{6+}$, 869.7 for $[M+5H]^{5+}$, 1086.8 for $[M+4H]^{4+}$.C) 218_240pi. The calculated molecular mass is 4139.08 and 592.3 for $[M+7H]^{7+}$, 690.8 for $[M+6H]^{6+}$, 828.8 for $[M+5H]^{5+}$, 1035.8 for $[M+4H]^{4+}$. D) 218_240piFar. The calculated molecular mass is 4343.26 and 621.5 for $[M+7H]^{7+}$, 724.9 for $[M+6H]^{6+}$, 869.7 for $[M+5H]^{5+}$, 1086.8 for $[M+4H]^{4+}$. E) 210_218pi. The calculated molecular mass is 4139.08 and 592.3 for $[M+7H]^{7+}$, 690.8 for $[M+6H]^{6+}$, 828.8 for $[M+5H]^{5+}$, 1035.8 for $[M+4H]^{4+}$. F) 210_218piFar. The calculated molecular mass is 4343.26 and 621.5 for $[M+7H]^{7+}$, 724.9 for $[M+6H]^{6+}$, 869.7 for $[M+5H]^{5+}$, 1086.8 for $[M+4H]^{4+}$.
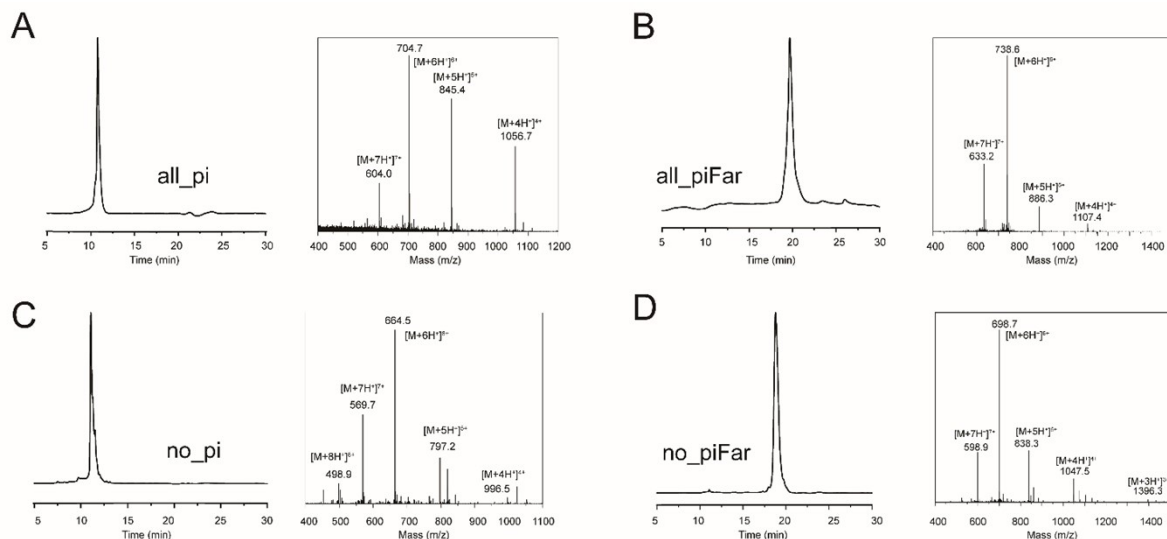
Figure S3. The analytical HPLC and ESI-MS analysis of synthesized none-phosphorylated and triple-phosphorylated Rnd peptides. All the peptides were analyzed by C18 analytical column, a gradient of 20-80% B (phase A solvent is distilled water with 0.6‰ TFA, phase B solvent is 80% acetonitrile in water with 0.6‰ TFA) for 30 min. A) all_pi. The calculated molecular mass is 4219.04 and 603.7 for $[M+7H]^{7+}$, 704.2 for $[M+6H]^{6+}$, 844.8 for $[M+5H]^{5+}$, 1055.8 for $[M+4H]^{4+}$. B) all_piFar. The calculated molecular mass is 4423.23 and 632.89 for $[M+7H]^{7+}$, 738.2 for $[M+6H]^{6+}$, 885.6 for $[M+5H]^{5+}$, 1106.8 for $[M+4H]^{4+}$. C) no_pi. The calculated molecular mass is 3979.14 and 498.4 for $[M+8H]^{8+}$, 569.4 for $[M+7H]^{7+}$, 664.2 for $[M+6H]^{6+}$, 796.8 for $[M+5H]^{5+}$, 995.8 for $[M+4H]^{4+}$. D) no_piFar. The calculated molecular mass is 4183.33 and 598.6 for $[M+7H]^{7+}$, 698.2 for $[M+6H]^{6+}$, 837.7 for $[M+5H]^{5+}$, 1046.8 for $[M+4H]^{4+}$, 1395.4 for $[M+3H]^{3+}$,
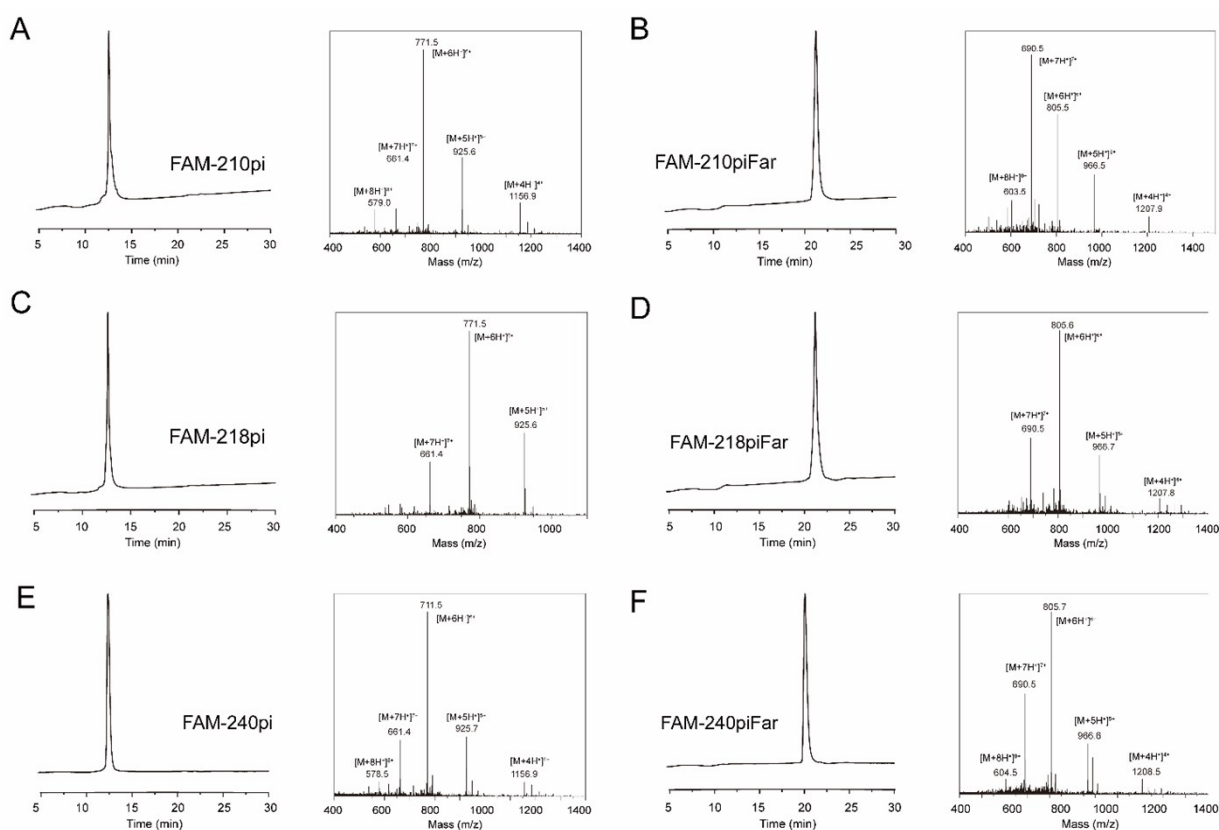

Figure S4. The analytical HPLC and ESI-MS analysis of synthesized single-phosphorylated Rnd3 peptides labeled with

carboxyfluorescein (FAM). All the peptides were analyzed by C18 analytical column, a gradient of 20-80% B (phase A solvent is distilled water with 0.6‰ TFA, phase B solvent is 80% acetonitrile in water with 0.6‰ TFA) for 30 min. A) FAM-210pi. The calculated molecular mass is 4620.27 and 578.5 for [M+8H]$^{8+}$, 661.0 for [M+7H]$^{7+}$, 771.0 for [M+6H]$^{6+}$, 925.1 for [M+5H]$^{5+}$, 1156.1 for [M+4H]$^{4+}$. B) FAM-210piFar. The calculated molecular mass is 4824.46 and 604.1 for [M+8H]$^{8+}$, 690.2 for [M+7H]$^{7+}$, 805.1 for [M+6H]$^{6+}$, 965.9 for [M+5H]$^{5+}$, 1207.1 for [M+4H]$^{4+}$. C) FAM-218pi. The calculated molecular mass is 4620.27 and 578.5 for [M+8H]$^{8+}$, 661.0 for [M+7H]$^{7+}$, 771.0 for [M+6H]$^{6+}$, 925.1 for [M+5H]$^{5+}$, 1156.1 for [M+4H]$^{4+}$. D) FAM-218piFar. The calculated molecular mass is 4824.46 and 690.2 for [M+7H]$^{7+}$, 805.1 for [M+6H]$^{6+}$, 965.9 for [M+5H]$^{5+}$, 1207.1 for [M+4H]$^{4+}$. E) FAM-240pi. The calculated molecular mass is 4620.27 and 578.5 for [M+8H]$^{8+}$, 661.0 for [M+7H]$^{7+}$, 771.0 for [M+6H]$^{6+}$, 925.1 for [M+5H]$^{5+}$, 1156.1 for [M+4H]$^{4+}$. F) FAM-240piFar. The calculated molecular mass is 4824.46 and 604.1 for [M+8H]$^{8+}$, 690.2 for [M+7H]$^{7+}$, 805.1 for [M+6H]$^{6+}$, 965.9 for [M+5H]$^{5+}$, 1207.1 for [M+4H]$^{4+}$.
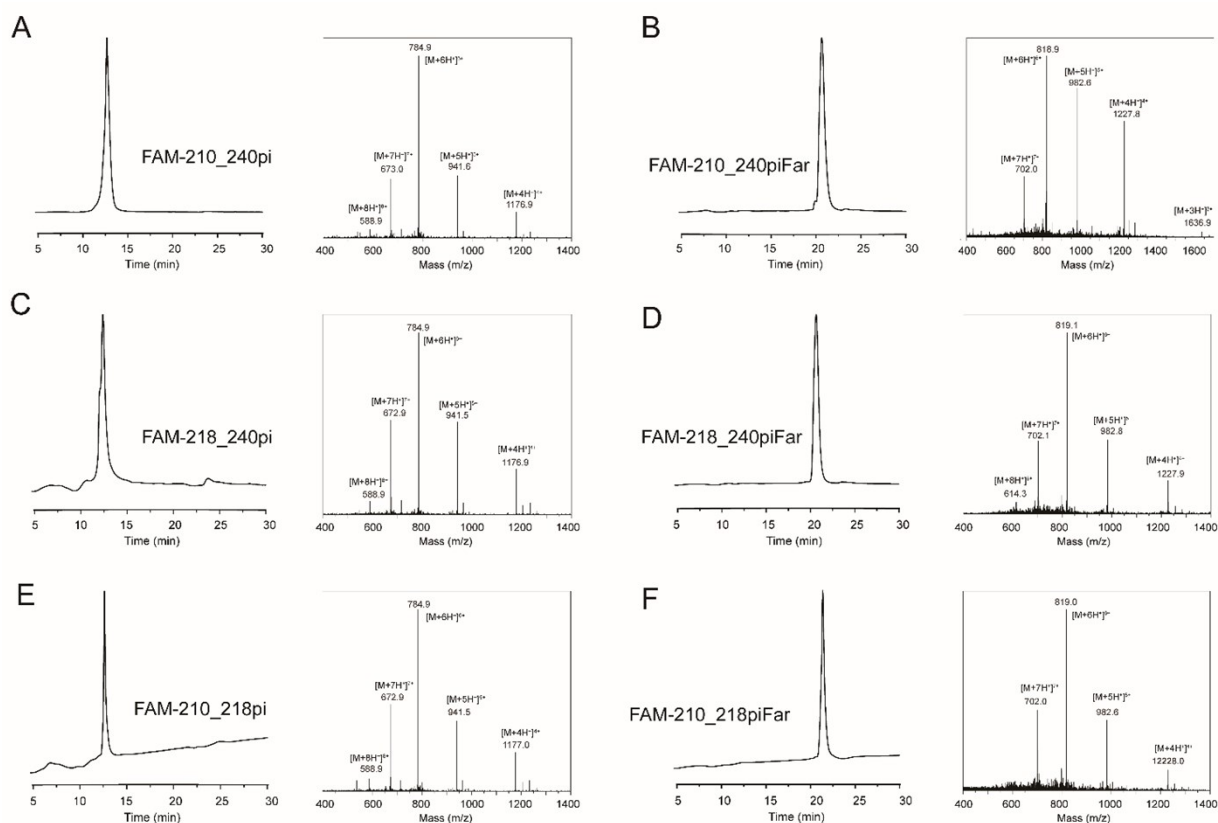

Figure S5. The analytical HPLC and ESI-MS analysis of synthesized dual-phosphorylated Rnd3 peptides labeled with carboxyfluorescein (FAM). All the peptides were analyzed by C18 analytical column, a gradient of 20-80% B (phase A solvent is distilled water with 0.6‰ TFA, phase B solvent is 80% acetonitrile in water with 0.6‰ TFA) for 30 min. A) FAM-210_240pi. The calculated molecular mass is 4700.24 and 588.5 for [M+8H]$^{8+}$, 672.5 for [M+7H]$^{7+}$, 784.4 for [M+6H]$^{6+}$, 941.0 for [M+5H]$^{5+}$, 1176.1 for [M+4H]$^{4+}$. B) FAM-210_240piFar. The calculated molecular mass is 4904.43 and 701.6 for [M+7H]$^{7+}$, 818.4 for [M+6H]$^{6+}$, 981.9 for [M+5H]$^{5+}$, 1227.1 for [M+4H]$^{4+}$. C) FAM-218_240pi. The calculated molecular mass is 4700.24 and 588.5 for [M+8H]$^{8+}$, 672.5 for [M+7H]$^{7+}$, 784.4 for [M+6H]$^{6+}$, 941.0 for [M+5H]$^{5+}$, 1176.1 for [M+4H]$^{4+}$. D) FAM-218_240piFar. The calculated molecular mass is 4904.43 and 614.1 for [M+8H]$^{8+}$, 701.6 for [M+7H]$^{7+}$, 818.4 for [M+6H]$^{6+}$, 981.9 for [M+5H]$^{5+}$, 1227.1 for [M+4H]$^{4+}$. E) FAM-210_218pi. The calculated molecular mass is 4700.24 and 588.5 for [M+8H]$^{8+}$, 672.5 for [M+7H]$^{7+}$, 784.4 for [M+6H]$^{6+}$, 941.0 for [M+5H]$^{5+}$, 1176.1 for [M+4H]$^{4+}$. F) FAM-210_218piFar. The calculated molecular mass is 4904.43 and 701.6 for [M+7H]$^{7+}$, 818.4 for [M+6H]$^{6+}$, 981.9 for [M+5H]$^{5+}$, 1227.1 for [M+4H]$^{4+}$.
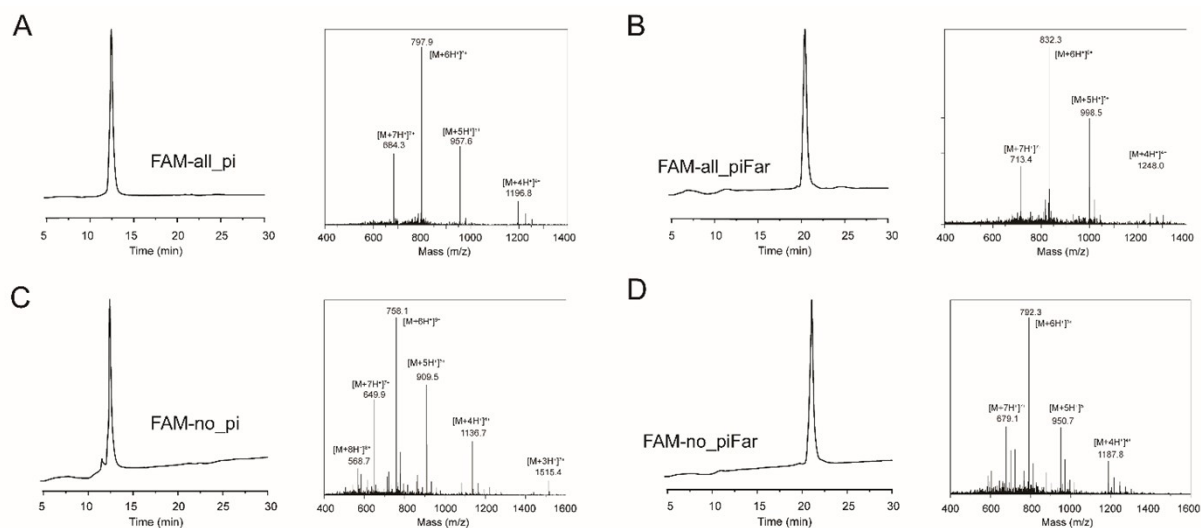
Figure S6. The analytical HPLC and ESI-MS analysis of synthesized none-phosphorylated and triple-phosphorylated Rnd peptides labeled with carboxyfluorescein (FAM). All the peptides were analyzed by C18 analytical column, a gradient of 20-80% B (phase A solvent is distilled water with 0.6‰ TFA, phase B solvent is 80% acetonitrile in water with 0.6‰ TFA) for 30 min. A) FAM-all_pi. The calculated molecular mass is 4780.21 and 683.9 for $[M+7H]^{7+}$, 797.7 for $[M+6H]^{6+}$, 957.0 for $[M+5H]^{5+}$, 1196.1 for $[M+4H]^{4+}$. B) FAM-all_piFar. The calculated molecular mass is 4984.39 and 713.1 for $[M+7H]^{7+}$, 831.7 for $[M+6H]^{6+}$, 997.9 for $[M+5H]^{5+}$, 1247.1 for $[M+4H]^{4+}$. C) FAM-no_pi. The calculated molecular mass is 4540.31 and 568.5 for $[M+8H]^{8+}$, 649.6 for $[M+7H]^{7+}$, 757.1 for $[M+6H]^{6+}$, 909.1 for $[M+5H]^{5+}$, 1136.1 for $[M+4H]^{4+}$, 1514.4.1 for $[M+3H]^{3+}$. D) FAM-no_piFar. The calculated molecular mass is 4744.49 and 678.8 for $[M+7H]^{7+}$, 791.7 for $[M+6H]^{6+}$, 949.9 for $[M+5H]^{5+}$, 1187.1 for $[M+4H]^{4+}$.
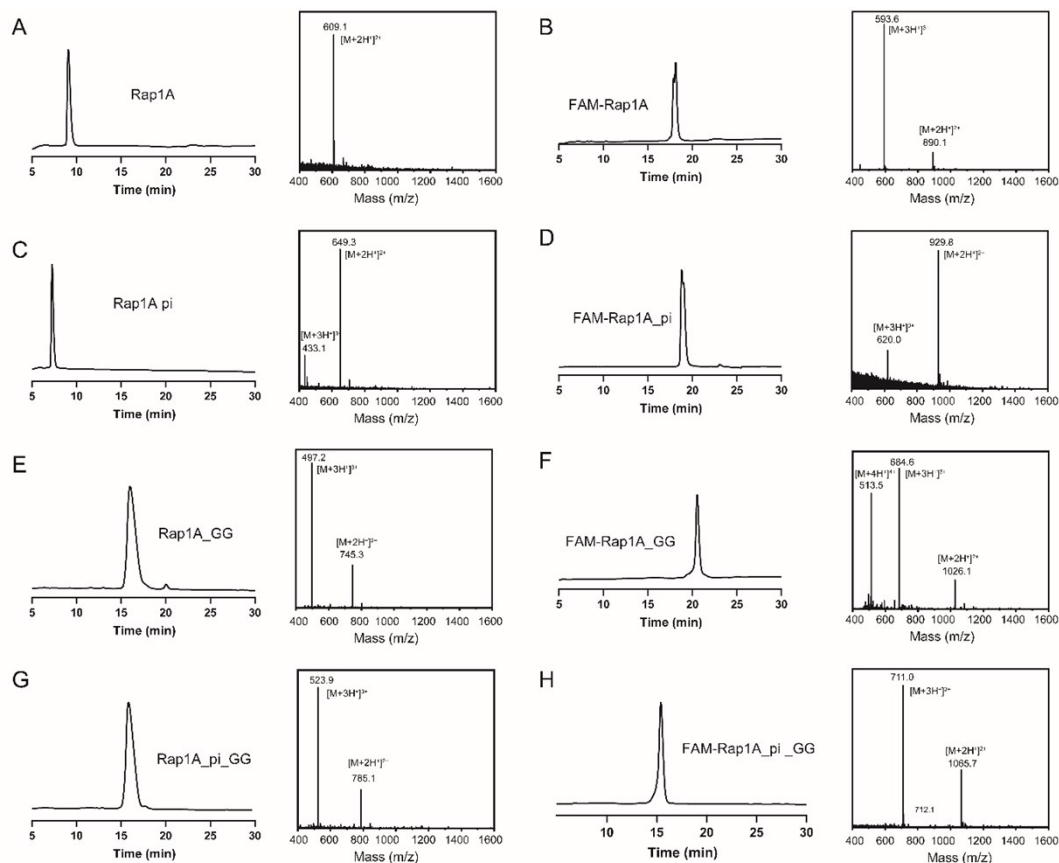
Figure S7. The analytical HPLC and ESI-MS analysis of synthesized Rap1A peptides. All the peptides were analyzed by C18 analytical column, for A-D) a gradient of 5-50% B, E-H) a gradient of 30-80% B (phase A solvent is distilled water with 0.6‰ TFA, phase B solvent is 80% acetonitrile in water with 0.6‰ TFA) for 30 min. A) Rap1A. The calculated molecular mass is 1216.73 and 609.365 for $[M+2H]^{2+}$. B) FAM-Rap1A. The calculated molecular mass is 1777.90 and 889.95 for $[M+2H]^{2+}$, 593.6 for $[M+3H]^{3+}$. C) Rap1A_pi. The calculated molecular mass is 1296.70 and 649.35 for $[M+2H]^{2+}$, 433.2 for $[M+3H]^{3+}$. D) FAM-Rap1A_pi. The calculated molecular mass is 1857.86 and 929.93 for $[M+2H]^{2+}$, 620.3 for $[M+3H]^{3+}$. E) Rap1A_GG. The calculated molecular mass is 1488.98 and 745.5 for $[M+2H]^{2+}$, 497.3 for $[M+3H]^{3+}$. F) FAM-Rap1A_GG. The calculated molecular mass is 2050.15 and 1026.1 for $[M+2H]^{2+}$, 684.4 for $[M+3H]^{3+}$, 513.5 for $[M+4H]^{4+}$. G) Rap1A_pi_GG. The calculated molecular mass is 1568.95 and 785.5 for $[M+2H]^{2+}$, 524.0 for $[M+3H]^{3+}$. H) FAM-Rap1A_pi_GG. The calculated molecular mass is 2130.11 and 1066.0 for $[M+2H]^{2+}$, 711.0 for $[M+3H]^{3+}$.
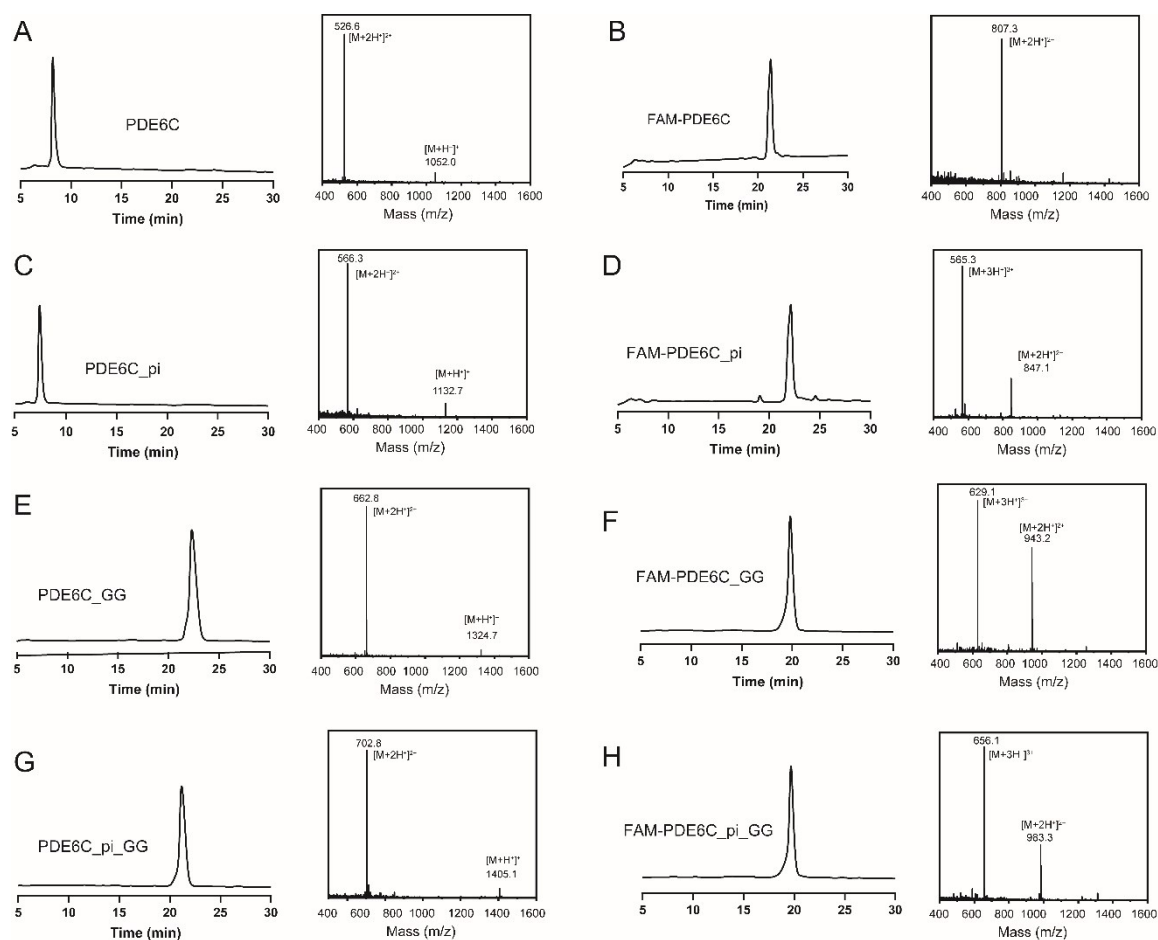

Figure S8. The analytical HPLC and ESI-MS analysis of synthesized PDE6C peptides. All the peptides were analyzed by C18 analytical column, for A-D) a gradient of 5-50% B, E-H) a gradient of 30-80% B (phase A solvent is distilled water with 0.6‰ TFA, phase B solvent is 80% acetonitrile in water with 0.6‰ TFA) for 30 min. A) PDE6C. The calculated molecular mass is 1051.50 and 1052.5 for $[M+H]^{+}$, 526.7 for $[M+2H]^{2+}$. B) FAM-PDE6C. The calculated molecular mass is 1612.66 and 807.3 for $[M+2H]^{2+}$. C) PDE6C_pi. The calculated molecular mass is 1131.46 and 1132.5 for $[M+H]^{+}$, 566.7 for $[M+2H]^{2+}$. D) FAM-PDE6C_pi. The calculated molecular mass is 1692.63 and 847.3 for $[M+2H]^{2+}$, 565.2 for $[M+3H]^{3+}$. E) PDE6C_GG. The calculated molecular mass is 1323.75 and 1324.7 for $[M+H]^{+}$, 662.9 for $[M+2H]^{2+}$. F) FAM-PDE6C_GG. The calculated molecular mass is 1884.91 and 943.4 for $[M+2H]^{2+}$, 629.3 for $[M+3H]^{3+}$. G) PDE6C_pi_GG. The calculated molecular mass is 1403.71 and 1404.7 for $[M+H]^{+}$, 702.8 for $[M+2H]^{2+}$. H) FAM-PDE6C_pi_GG. The calculated molecular mass is 1964.88 and 983.4 for $[M+2H]^{2+}$, 656.0 for $[M+3H]^{3+}$.
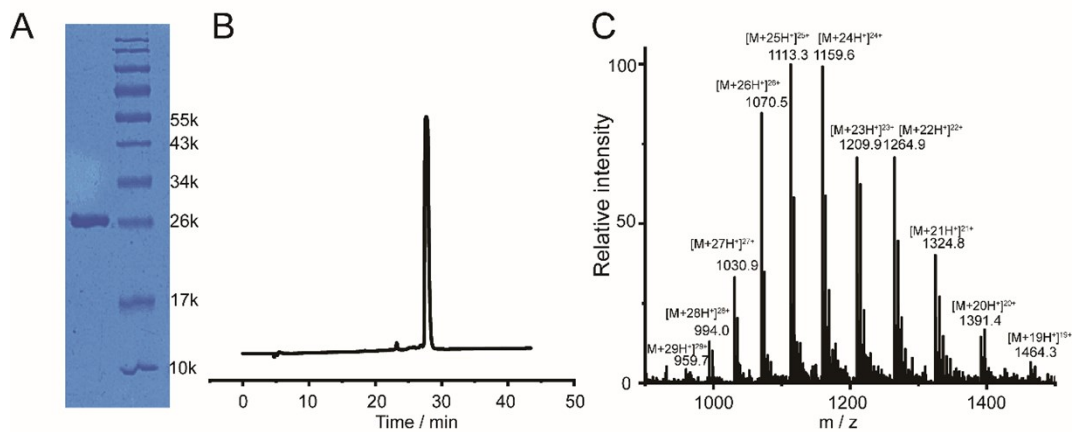
Figure S9. Characterization of 14-3-3ζ. A) SDS-PAGE of 14-3-3ζ. B) Analytical HPLC of 14-3-3ζ. C) ESI-MS of 14-3-3ζ. The calculated molecular weight is 27802.16, and 959.7 for $[M+29H]^{29+}$, 993.9 for $[M+28H]^{28+}$, 1030.7 for $[M+27H]^{27+}$, 1070.3 for $[M+26H]^{26+}$, 1113.1 for $[M+25H]^{25+}$, 1159.4 for $[M+24H]^{24+}$, 1209.8 for $[M+23H]^{23+}$, 1274.7 for $[M+22H]^{22+}$, 1324.9 for $[M+21H]^{21+}$, 1391.1 for $[M+20H]^{20+}$, 1464.3 for $[M+19H]^{19+}$.
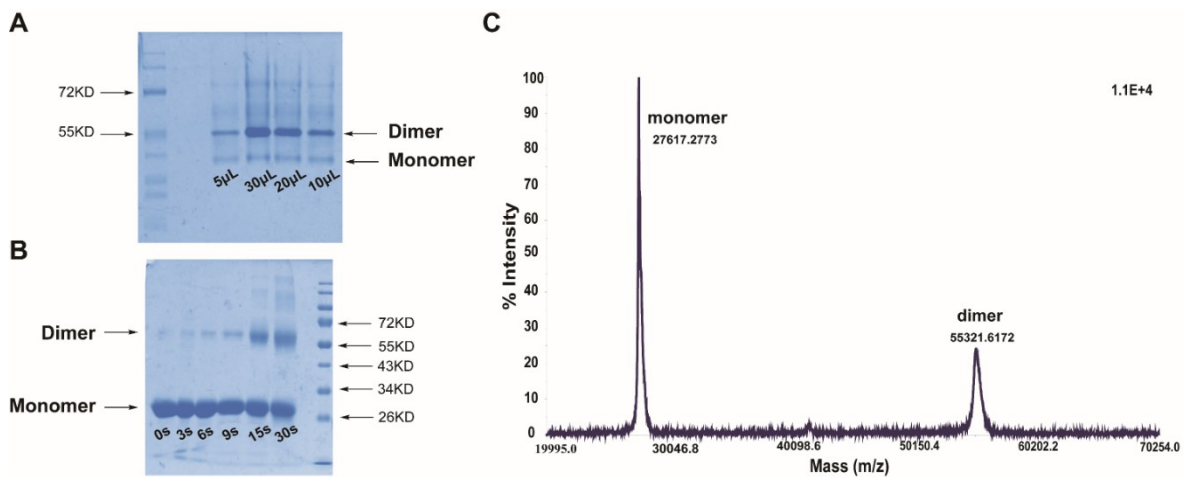

Figure S10. Characterization of the formation of 14-3-3ζ dimer. A) The Native PAGE of 14-3-3ζ with different loading quantities. The lane on the far left is Prestained Protein Ladder. B) The SDS-PAGE of photo-crosslined 14-3-3ζ with different crosslinking time. The lane on the far right is Prestained Protein Ladder. C) The MALDI-TOF of 14-3-3ζ.
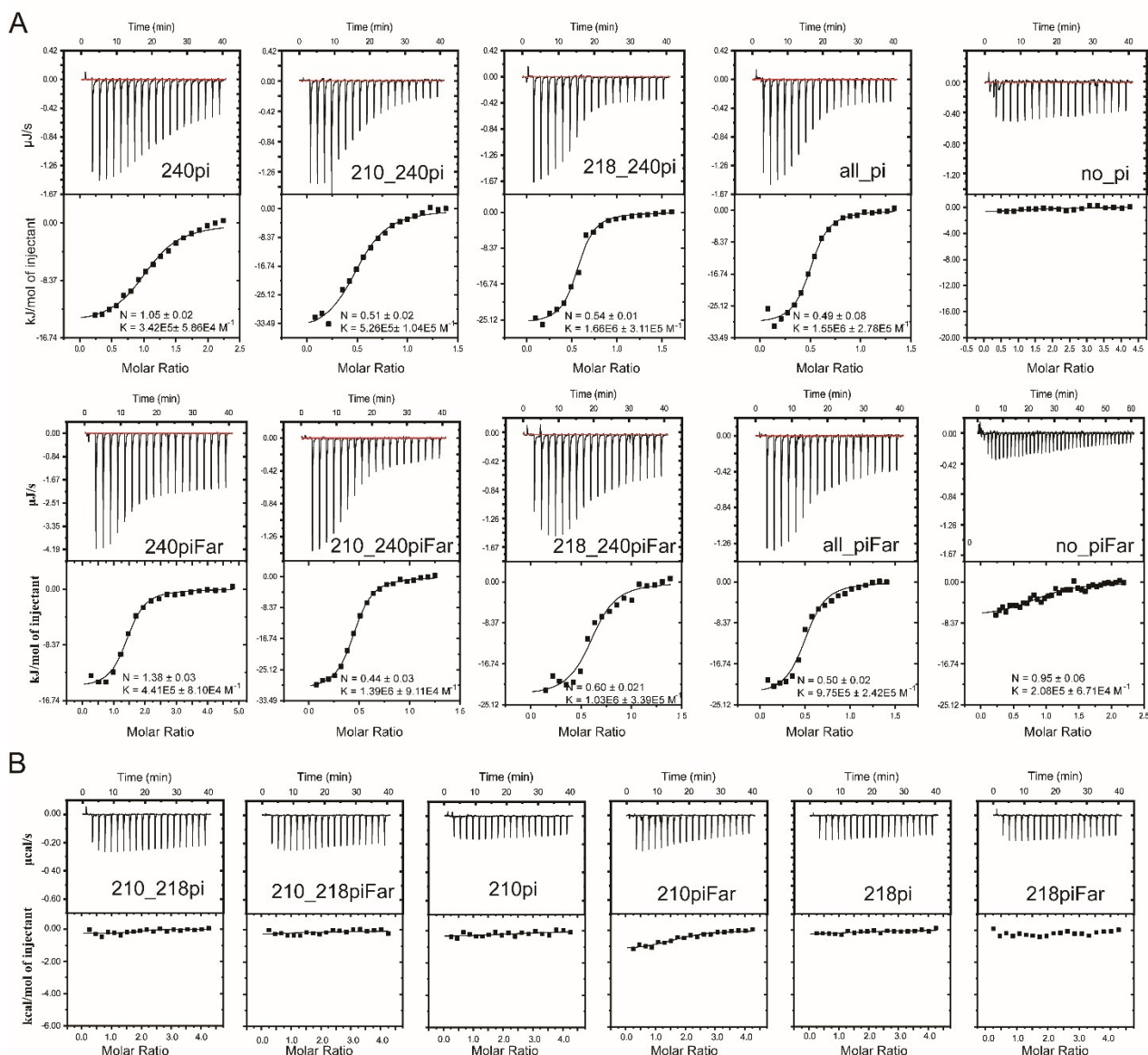
11

Figure S11. ITC titrations of Rnd3 peptides with 14-3-3ζ. All the experiments were performed at 25 °C. Singly phosphorylated peptides (400 µM) and multiphosphorylated peptides (200 µM) were titrated into 40 µM 14-3-3ζ. N represents the binding radio of peptides to 14-3-3ζ. K represents the association constant.
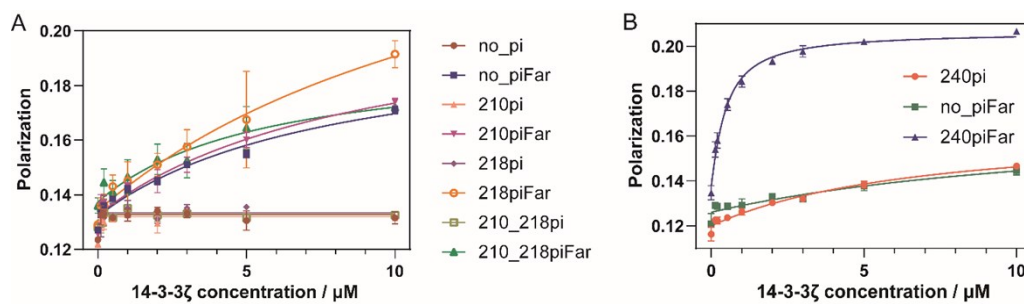

Figure S12. Fluorescence polarization assay of FAM-labeled Rnd3 peptides with 14-3-3ζ. The concentration of each FAM-labeled Rnd3 peptide was 250 nM. For peptide 240pi, K_D = 3.39 ± 0.02 µM; for peptide nopi_Far, K_D = 7.74 ± 4.16 µM, for peptide 240piFar, K_D = 0.32 ± 0.01 µM. The plots are the mean values ± SD (error bars) of four independent measurements.
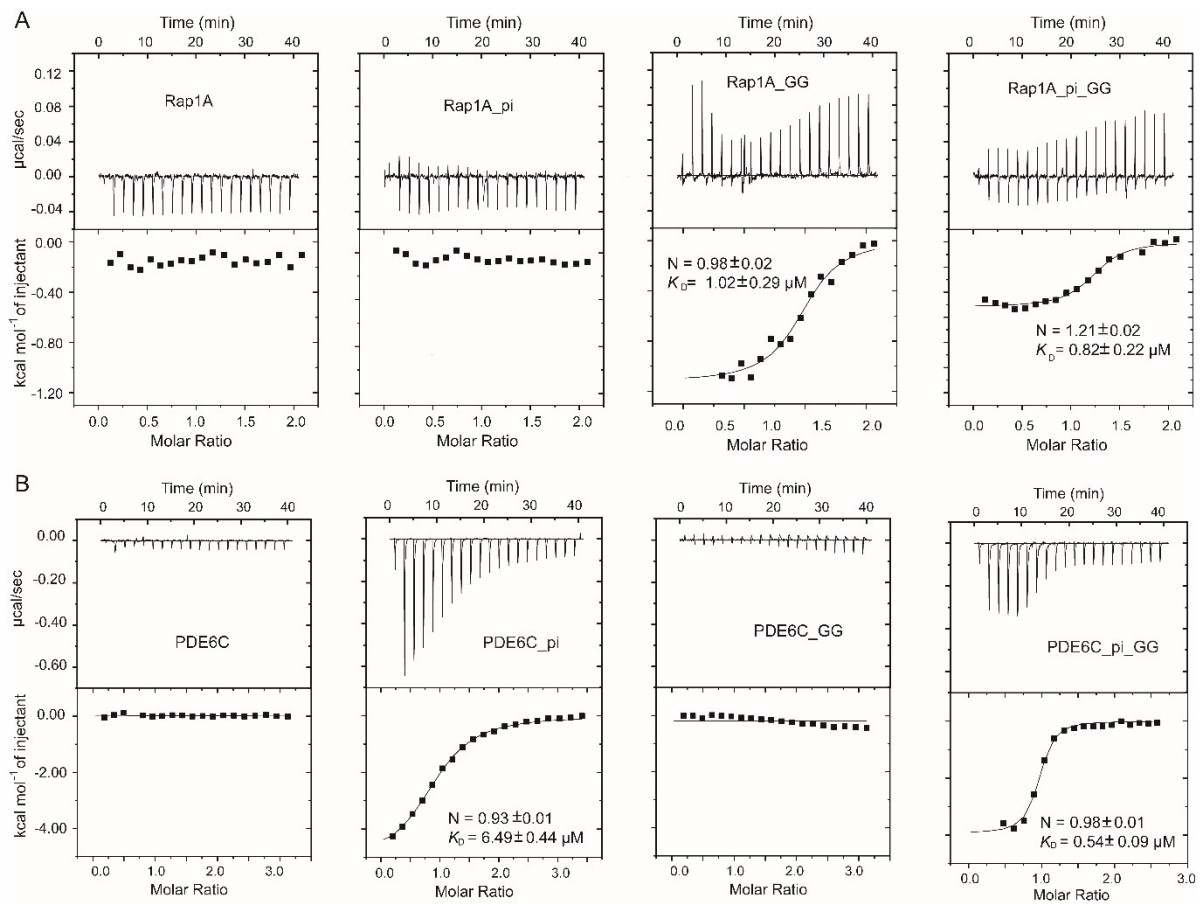
Figure S13. ITC titrations of Rap1A and PDE6C peptides with 14-3-3ζ. All the experiments were performed at 25 °C. Different modified peptides (400 μM) were titrated into 40 μM 14-3-3ζ. N represents the binding radio of peptides to 14-3-3ζ. K_D represents the association constant.
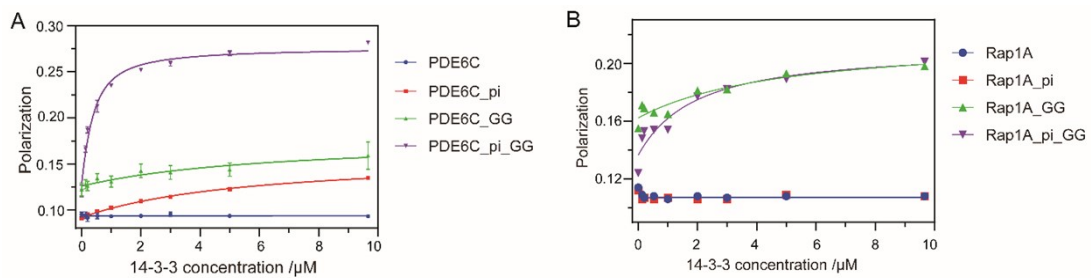

Figure S14. Fluorescence polarization assay of FAM-labeled PDE6C and Rap1A peptides with 14-3-3ζ. The concentration of each FAM-labeled peptide was 250 nM. The plots are the mean values ± SD (error bars) of three independent measurements. For peptide PDE6C_pi, K_D = 5.51 ± 1.51 μM; for peptide PDE6C_pi_GG, K_D = 0.27 ± 0.09 μM
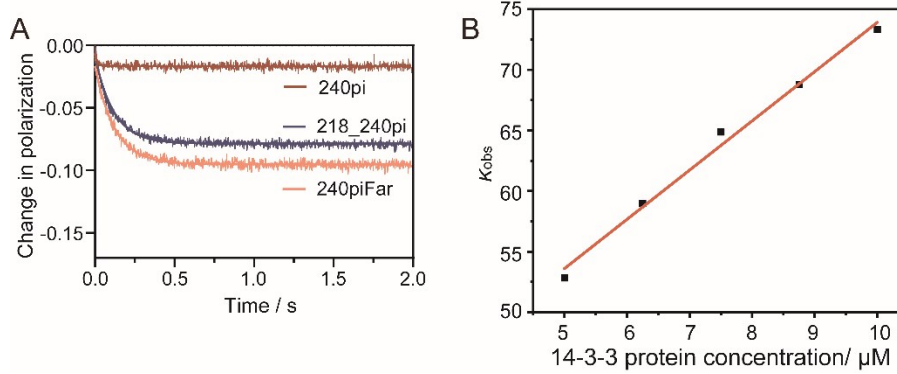
Figure S15. The kinetic data of Rnd3 and PDE6C peptides with different modified patterns and 14-3-3ζ. A) Dissociation curves of FAM labeled Rnd3 peptides from 14-3-3ζ after the addition of competitive label-free peptides measured in a stopped-flow apparatus coupled with a FP detector. The curve was fitted with a one-phase exponential decay model to give the $k_{d,ov}$. 240pi is 63.92 s^{-1}, 240piFar is 8.02 s^{-1}, 218_240pi is 8. 42 s^{-1}. B) The observed rate constant of PDE6C_pi with increasing concentration of 14-3-3ζ. The curves in figure 6D in the manuscript were fitted with single exponential function to give the k_{obs}. Assuming the association reactions is one-step reversible interaction, thus, $k_{obs} = k_{on} * [14\text{-}3\text{-}3ζ] + k_{off}$. The calculated k_{on} = 4.06 μM^{-1}s^{-1}, k_{off} = 33.29 s^{-1}.
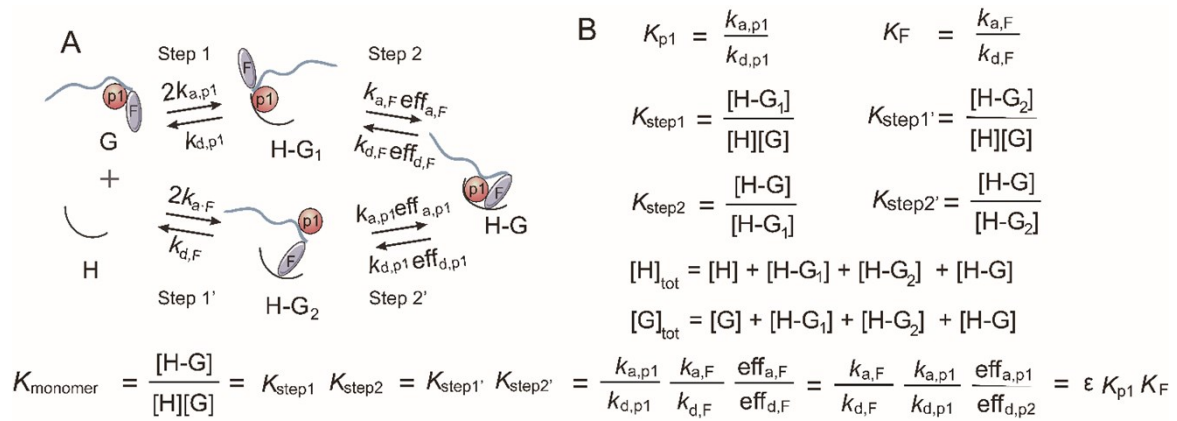

Figure S16. The thermodynamic and kinetics model of phosphorylated and farnesylated peptide binding with 14-3-3ζ monomer. The binding process is divided into two steps. Guest (G) represents Rnd3 peptides and host (H) represents 14-3-3ζ monomer. The complex H-G$_1$, H-G$_2$ represent monovalent binding and complex H-G represent the final binding. $k_{a,p1}$ is the association rate constant of peptide bearing phosphorylation at S240 with 14-3-3ζ. $k_{d,p1}$ is the dissociation rate constant of peptide bearing the phosphorylation at S240 with 14-3-3ζ. $eff_{a,xx}$ is the degree to which the association process in the second binding step is affected by the one in the first binding step; $eff_{d,xx}$ is the degree to which the dissociation process in the second binding step is affected by the first binding event. p1 in orange represents pS240 in Rnd3 peptide, F in grey represents farnesyl group in Rnd3 peptide. B) Mass action laws and mass balance equations for the interaction. K is the association constant.

$$H + G \underset{k_{d,1}}{\overset{k_{a,1}}{\rightleftharpoons}} H\text{-}G_* \underset{k_{d,2}}{\overset{k_{a,2}}{\rightleftharpoons}} H\text{-}G$$

initial concentration: a   b   0   0

concentration at time t: a-m-n   b-m-n   m   n

$$\frac{d[H]}{dt} = k_{d,1}[H\text{-}G_*] - k_{a,1}[H][G] \qquad\qquad \frac{d(a\text{-}m\text{-}n)}{dt} = k_{d,1}*m - k_{a,1}*(a\text{-}m\text{-}n)(b\text{-}m\text{-}n)$$

$$\frac{d[G]}{dt} = k_{d,1}[H\text{-}G_*] - k_{a,1}[H][G] \qquad\qquad \frac{d(b\text{-}m\text{-}n)}{dt} = k_{d,1}*m - k_{a,1}*(a\text{-}m\text{-}n)(b\text{-}m\text{-}n)$$

$$\frac{d[H\text{-}G]}{dt} = k_{a,2}[H\text{-}G_*] - k_{d,2}[H][G] \qquad\qquad \frac{dn}{dt} = k_{a,2}*m - k_{d,2}*n$$

$$\frac{d[H\text{-}G_*]}{dt} = k_{a,1}[H][G] + k_{d,2}[H\text{-}G] - (k_{a,2}+ k_{d,1})[H\text{-}G_*] \qquad \frac{dm}{dt} = k_{a,1}*(a\text{-}m\text{-}n)(b\text{-}m\text{-}n) + k_{d,2}*n - (k_{a,2}+ k_{d,1})m$$

$$y = r_0*[G] + r_1*[H\text{-}G_*] + r_2*[H\text{-}G] + \text{offset} \qquad\qquad y = r_0*(b\text{-}m\text{-}n) + r_1*m + r_2*n + C$$
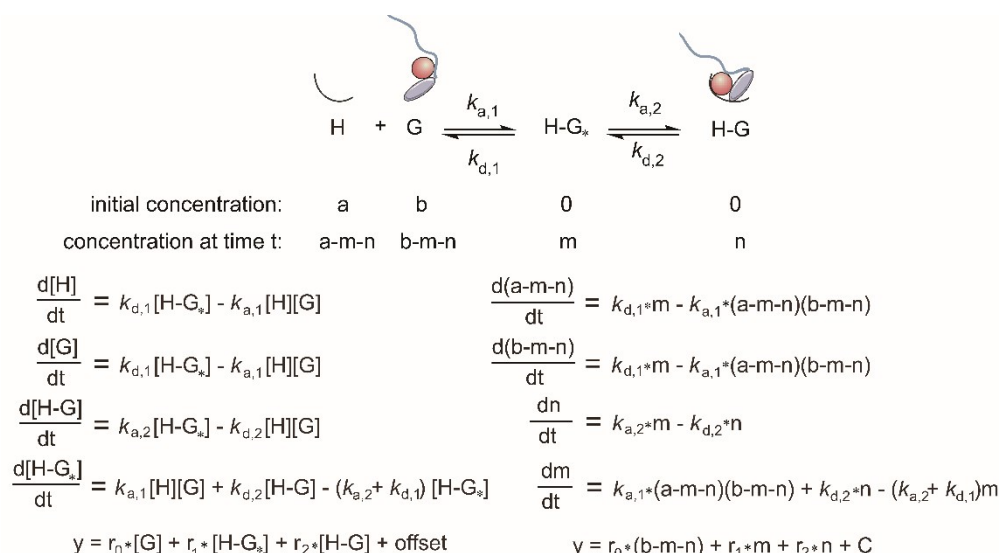
Figure S17. The kinetic equations described the two-step binding process. G represents the Rnd3 peptides and H represents 14-3-3ζ. y was defined as the fluorescence polarization. r_0 defined as the polarization coefficient of G, r_1 defined as the polarization coefficient of H-G$_*$, r_2 defined as the polarization coefficient of H-G.
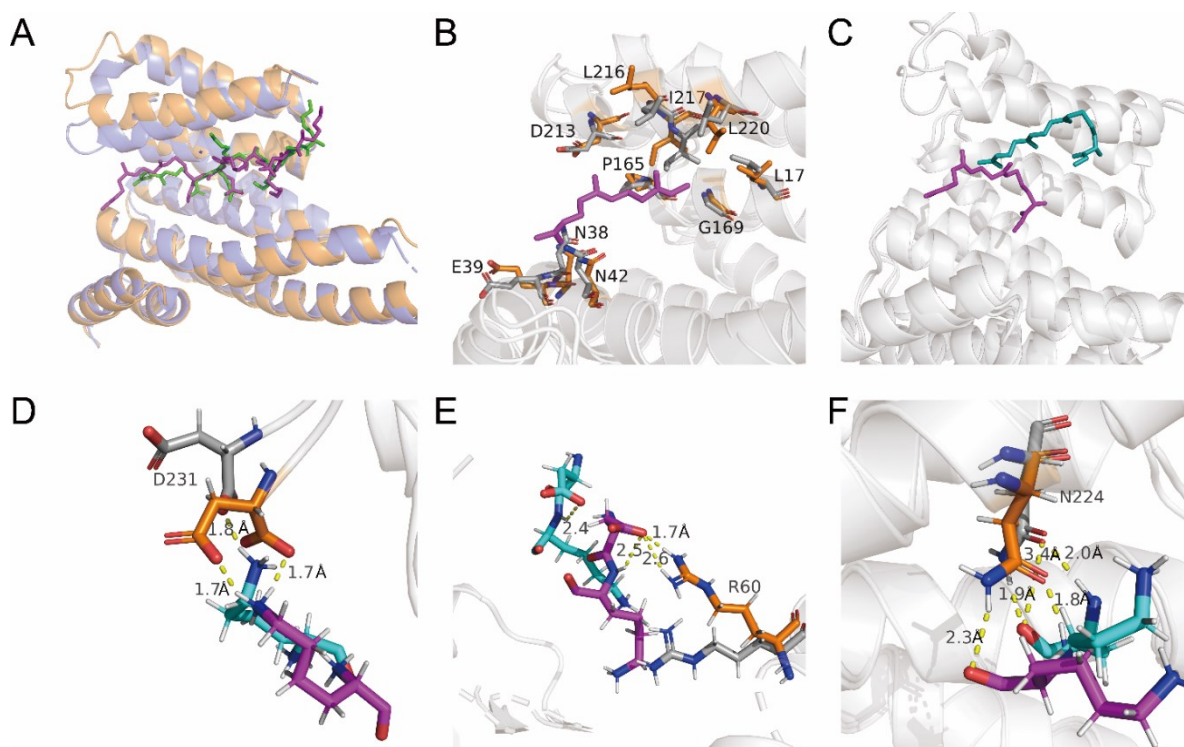

Figure S18. The most frequently occurring structures of MD. A) The compared structure of 14-3-3ζ bound with 240piFar and crystal structure earlier reported[5]. Structure we simulated is orange, the crystal structure is slate. The peptide in green is the ligand for crystal structure and the peptide in magenta is the ligand we simulated. B) Residues in 14-3-3ζ compared when 14-3-3ζ bound with peptide 240pi and 240piFar. C) Farnesyl group binding pocket compared when 14-3-3ζ bound with peptide no_piFar and 240piFar. D) Comparison of K235 in Rnd3 peptide interacted with 14-3-3ζ residues. E) Comparison of D236 in Rnd3 peptide interacted with 14-3-3ζ residues. F) Comparison of K239 in Rnd3 peptide interacted with 14-3-3ζ residues. 240piFar peptide is magenta, 240pi peptide is cyan, no_piFar peptide is teal. The residues of 14-3-3ζ bound with 240piFar peptide is orange. The residues of 14-3-3ζ bound with 240pi peptide is gray.
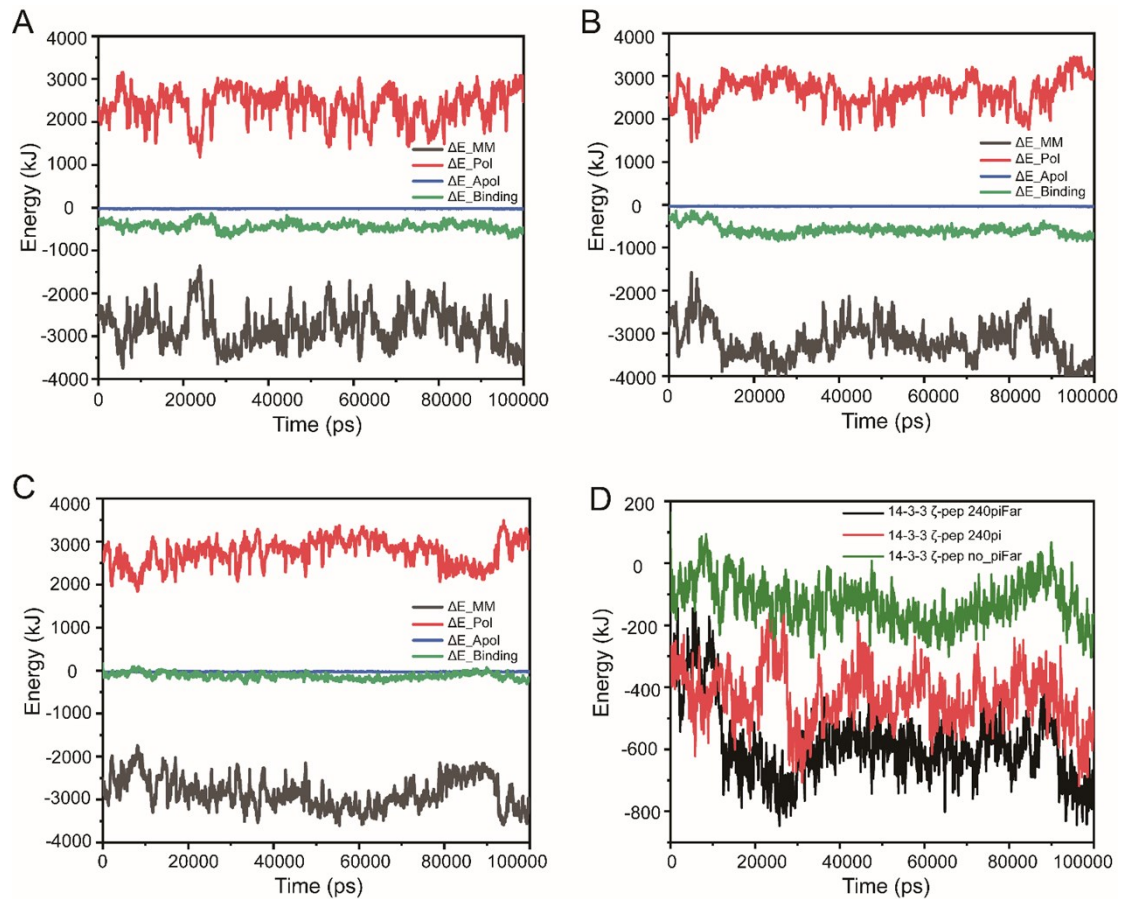
Figure S19. Changes in free energy of protein-peptide binding over time. A) with peptide 240pi. B) with peptide 240piFar. C) with peptide no_piFar. D) The comparison of binding free energy in three systems.
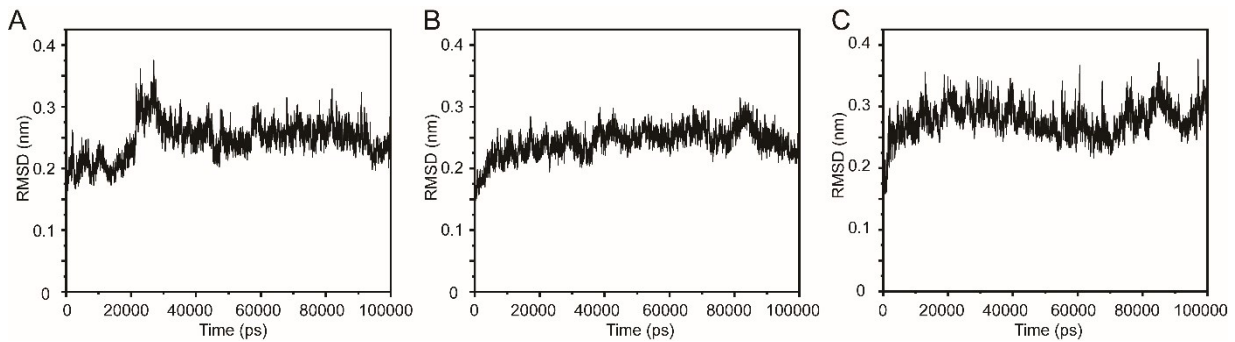

Figure S20. Changes in RMSD values of proteins in the three systems over time. A) with peptide 240pi. B) with peptide 240piFar. C) with peptide no_piFar.
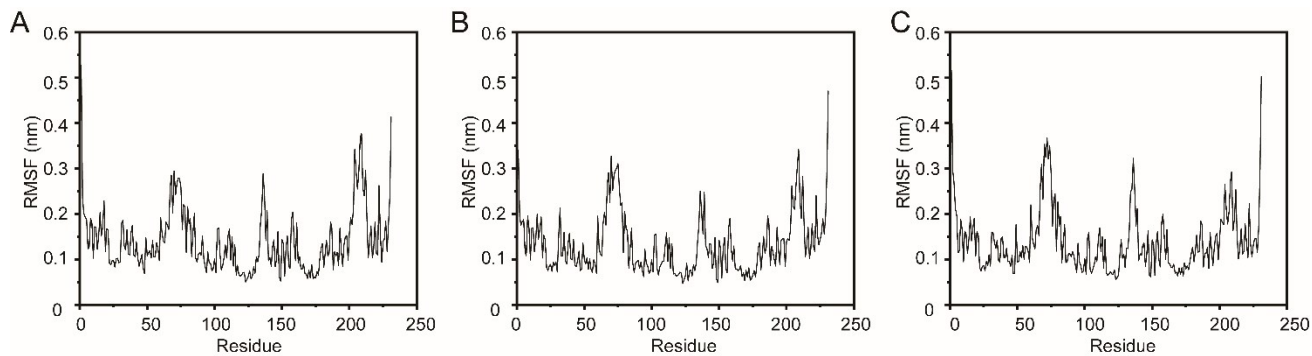
Figure S21. Changes in RMSF values of proteins in the three systems over time. A) with peptide 240pi. B) with peptide 240piFar. C) with peptide no_piFar.
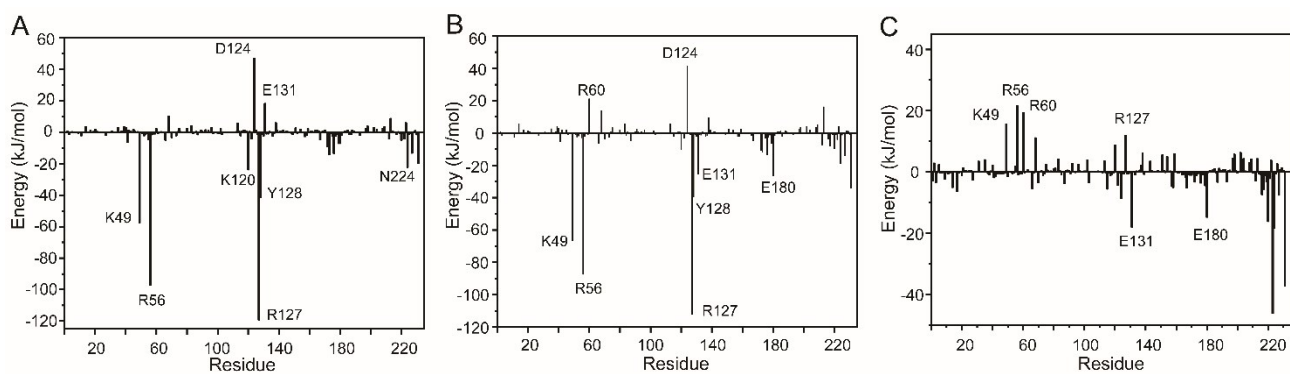

Figure S22. Energy contribution of amino acid residues to total binding energy on protein. A) with peptide 240pi. B) with peptide 240piFar. C) with peptide no_piFar.
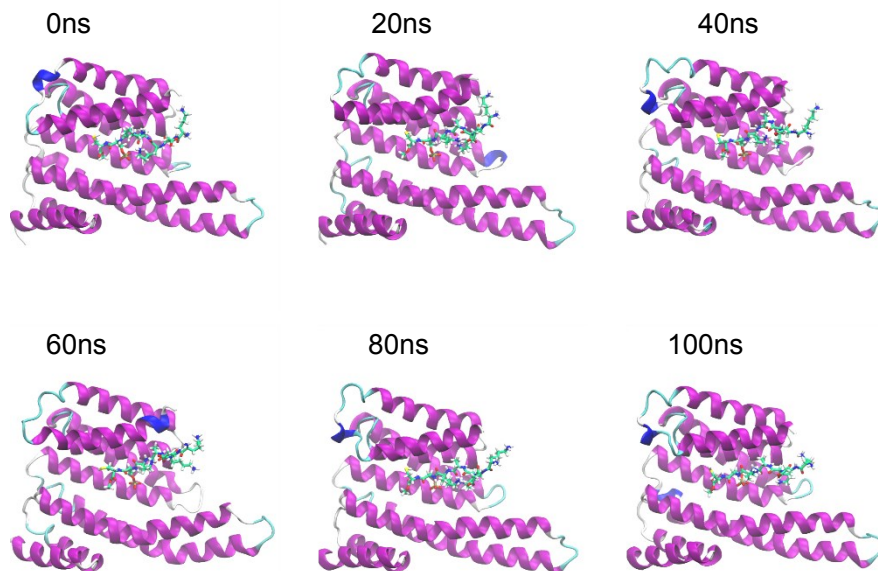

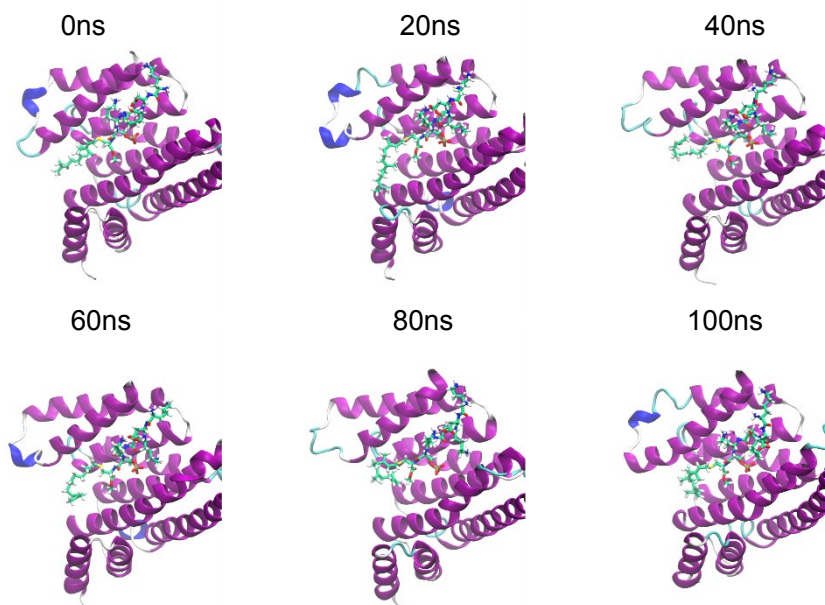Figure S23. Simulation results of 14-3-3ζ and peptide 240pi: images of structure in every 20 seconds.

0ns　　　20ns　　　40ns

60ns　　　80ns　　　100ns

Figure S24. Simulation results of 14-3-3ζ and peptide 240piFar: images of structure in every 20 seconds.

0ns　　　20ns　　　40ns

60ns　　　80ns　　　100ns
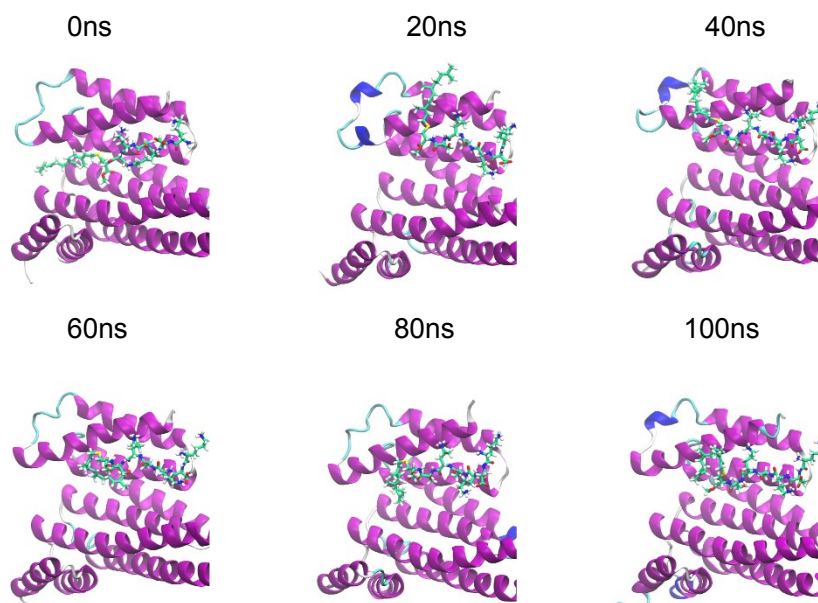
Figure S25. Simulation results of 14-3-3ζ and peptide no_piFar: images of structure in every 20 seconds.

Table S1. The sequence of synthesized Rnd3 peptides

Name	Peptide sequence
no_pi	H-RNKSQRATKRISHMPSRPELSAVATDLRKDKAKSC-OCH$_3$
No_piFar	H-RNKSQRATKRISHMPSRPELSAVATDLRKDKAKSC(Far)-OCH$_3$
210pi	H-RNKpSQRATKRISHMPSRPELSAVATDLRKDKAKSC-OCH$_3$
210piFar	H-RNKpSQRATKRISHMPSRPELSAVATDLRKDKAKSC(Far)-OCH$_3$
218pi	H-RNKSQRATKRIpSHMPSRPELSAVATDLRKDKAKSC-OCH$_3$
218piFar	H-RNKSQRATKRIpSHMPSRPELSAVATDLRKDKAKSC(Far)-OCH$_3$

240pi	H-RNKSQRATKRISHMPSRPELSAVATDLRKDKAKpSC-OCH$_3$
240piFar	H-RNKSQRATKRISHMPSRPELSAVATDLRKDKAKpSC(Far)-OCH$_3$
210_218pi	H-RNKpSQRATKRIpSHMPSRPELSAVATDLRKDKAKSC-OCH$_3$
210_218piFar	H-RNKpSQRATKRIpSHMPSRPELSAVATDLRKDKAKSC(Far)-OCH$_3$
218_240pi	H-RNKSQRATKRIpSHMPSRPELSAVATDLRKDKAKpSC-OCH$_3$
218_240piFar	H-RNKSQRATKRIpSHMPSRPELSAVATDLRKDKAKpSC(Far)-OCH$_3$
210_240pi	H-RNKpSQRATKRISHMPSRPELSAVATDLRKDKAKpSC-OCH$_3$
210_240piFar	H-RNKpSQRATKRISHMPSRPELSAVATDLRKDKAKpSC(Far)-OCH$_3$
all_pi	H-RNKpSQRATKRIpSHMPSRPELSAVATDLRKDKAKpSC-OCH$_3$
all_piFar	H-RNKpSQRATKRIpSHMPSRPELSAVATDLRKDKAKpSC(Far)-OCH$_3$
FAM-no_pi	FAM-NH-(CH$_2$CH$_2$O)$_3$-CH$_2$CH$_2$CO-RNKSQRATKRISHMPSRPELSAVATDLRKDKAKSC-OCH$_3$
FAM-no_piFar	FAM-NH-(CH$_2$CH$_2$O)$_3$-CH$_2$CH$_2$CO-RNKSQRATKRISHMPSRPELSAVATDLRKDKAKSC(Far)-OCH$_3$
FAM-210pi	FAM-NH-(CH$_2$CH$_2$O)$_3$-CH$_2$CH$_2$CO-RNKpSQRATKRISHMPSRPELSAVATDLRKDKAKSC-OCH$_3$
FAM-210piFar	FAM-NH-(CH$_2$CH$_2$O)$_3$-CH$_2$CH$_2$CO-RNKpSQRATKRISHMPSRPELSAVATDLRKDKAKSC(Far)-OCH$_3$
FAM-218pi	FAM-NH-(CH$_2$CH$_2$O)$_3$-CH$_2$CH$_2$CO-RNKSQRATKRIpSHMPSRPELSAVATDLRKDKAKSC-OCH$_3$
FAM-218piFar	FAM-NH-(CH$_2$CH$_2$O)$_3$-CH$_2$CH$_2$CO-RNKSQRATKRIpSHMPSRPELSAVATDLRKDKAKSC(Far)-OCH$_3$
FAM-240pi	FAM-NH-(CH$_2$CH$_2$O)$_3$-CH$_2$CH$_2$CO-RNKSQRATKRISHMPSRPELSAVATDLRKDKAKpSC-OCH$_3$
FAM-240piFar	FAM-NH-(CH$_2$CH$_2$O)$_3$-CH$_2$CH$_2$CO-RNKSQRATKRISHMPSRPELSAVATDLRKDKAKpSC(Far)-OCH$_3$
FAM-210_218pi	FAM-NH-(CH$_2$CH$_2$O)$_3$-CH$_2$CH$_2$CO-RNKpSQRATKRIpSHMPSRPELSAVATDLRKDKAKSC-OCH$_3$
FAM-210_218piFar	FAM-NH-(CH$_2$CH$_2$O)$_3$-CH$_2$CH$_2$CO-RNKpSQRATKRIpSHMPSRPELSAVATDLRKDKAKSC(Far)-OCH$_3$
FAM-218_240pi	FAM-NH-(CH$_2$CH$_2$O)$_3$-CH$_2$CH$_2$CO-RNKSQRATKRIpSHMPSRPELSAVATDLRKDKAKpSC-OCH$_3$
FAM-218_240piFar	FAM-NH-(CH$_2$CH$_2$O)$_3$-CH$_2$CH$_2$CO-RNKSQRATKRIpSHMPSRPELSAVATDLRKDKAKpSC(Far)-OCH$_3$
FAM-210_240pi	FAM-NH-(CH$_2$CH$_2$O)$_3$-CH$_2$CH$_2$CO-RNKpSQRATKRISHMPSRPELSAVATDLRKDKAKpSC-OCH$_3$
FAM-210_240piFar	FAM-NH-(CH$_2$CH$_2$O)$_3$-CH$_2$CH$_2$CO-RNKpSQRATKRISHMPSRPELSAVATDLRKDKAKpSC(Far)-OCH$_3$
FAM-all_pi	FAM-NH-(CH$_2$CH$_2$O)$_3$-CH$_2$CH$_2$CO-RNKpSQRATKRIpSHMPSRPELSAVATDLRKDKAKpSC-OCH$_3$
FAM-all_piFar	FAM-NH-(CH$_2$CH$_2$O)$_3$-CH$_2$CH$_2$CO-RNKpSQRATKRIpSHMPSRPELSAVATDLRKDKAKpSC(Far)-OCH$_3$
PDE6C	H-GGDDKKSKTC-OCH$_3$

PDE6C_pi	H-GGDDKKSKpTC-OCH$_3$
PDE6C_GG	H-GGDDKKSKTC(GG)-OCH$_3$
PDE6C_pi_GG	H-GGDDKKSKpTC(GG)-OCH$_3$
FAM-PDE6C	FAM-NH-(CH$_2$CH$_2$O)$_3$-CH$_2$CH$_2$COONH-GGDDKKSKTC-OCH3
FAM-PDE6C_pi	FAM-NH-(CH$_2$CH$_2$O)$_3$-CH$_2$CH$_2$COONH-GGDDKKSKpTC-OCH3
FAM-PDE6C_GG	FAM-NH-(CH$_2$CH$_2$O)$_3$-CH$_2$CH$_2$COONH-GGDDKKSKTC(GG)-OCH3
FAM-PDE6C_pi_GG	FAM-NH-(CH$_2$CH$_2$O)$_3$-CH$_2$CH$_2$COONH-GGDDKKSKpTC(GG)-OCH3
Rap1A	H-EKKKPKKKSC-OCH$_3$
Rap1A_pi	H-EKKKPKKKpSC-OCH$_3$
Rap1A_GG	H-EKKKPKKKSC(GG)-OCH$_3$
Rap1A_pi_GG	H-EKKKPKKKpSC(GG)-OCH$_3$
FAM- Rap1A	FAM-NH-(CH$_2$CH$_2$O)$_3$-CH$_2$CH$_2$COONH- EKKKPKKKSC-OCH$_3$
FAM- Rap1A_pi	FAM-NH-(CH$_2$CH$_2$O)$_3$-CH$_2$CH$_2$COONH- EKKKPKKKpSC-OCH$_3$
FAM- Rap1A_GG	FAM-NH-(CH$_2$CH$_2$O)$_3$-CH$_2$CH$_2$COONH- EKKKPKKKSC(GG)-OCH$_3$
FAM- Rap1A_pi_GG	FAM-NH-(CH$_2$CH$_2$O)$_3$-CH$_2$CH$_2$COONH- EKKKPKKKpSC(GG)-OCH$_3$

Tabel S2. The primer sequences we designed for the 14-3-3ζ-intein-CBD gene.

Primer name	Sequence
Primer F	GGAATTC**CATATG**GATAAAAACGAGCTGGTACAGAAGGC
Primer R	G**ACTAGT**GCATCTCCCGTGATGCATCCATTTTCCCCTC

3. References

1.   Zhang, S. Y.; Sperlich, B.; Li, F. Y.; Al-Ayoubi, S.; Chen, H. X.; Zhao, Y. F.; Li, Y. M.; Weise, K.; Winter, R.; Chen, Y. X., Phosphorylation Weakens but Does Not Inhibit Membrane Binding and Clustering of K-Ras4B. *ACS Chem. Biol.* **2017,** *12* (6), 1703-1710.

2.   Stocker, A.; Fretz, H.; Frick, H.;   Ruttimann, A.; Woggon, W. D., The substrate specificity of tocopherol cyclase. *Bioorg Med Chem* **1996,** *4* (7), 1129-34.

3.   Batjargal, S.; Walters, C. R.; Petersson, E. J., Inteins as traceless purification tags for unnatural amino acid proteins. *J. Am. Chem. Soc.* **2015,** *137* (5), 1734-7.

4.   Ono, K.; Condron, M. M.; Teplow, D. B., Structure–neurotoxicity relationships of amyloid β-protein oligomers. *Proc. Natl. Acad. Sci. USA* **2009,** *106* (35), 14745-14750.

5.   Riou, P.; Kjaer, S.; Garg, R.; Purkiss, A.; George, R.; Cain, R. J.; Bineva, G.; Reymond, N.; McColl, B.; Thompson, A. J.; O'Reilly, N.; McDonald, N. Q.;   Parker, P. J.; Ridley, A. J., 14-3-3 proteins interact with a hybrid prenyl-phosphorylation motif to inhibit G proteins. *Cell* **2013,** *153* (3), 640-53.